

# Flow Boiling Characteristics in Expanding Type Structured Heat Sinks for Different Roles of Gravitational Force

Burak Markal<sup>1</sup> and Alperen Evcimen<sup>2</sup>

<sup>1</sup>Department of Mechanical Engineering, Karadeniz Technical University  
61080, Trabzon, Türkiye

burakmarkal@ktu.edu.tr; alperen.evcimen@erdogan.edu.tr

<sup>2</sup>Department of Mechanical Engineering, Recep Tayyip Erdogan University  
53100, Rize, Türkiye

**Abstract** - The orientation of the devices that must be cooled can change depending on the application requirements. Orientation-based variations can influence the physical mechanism regarding the coolers. Therefore, here, saturated flow boiling in the structured (expanding micro pin-finned with staggered array) micro heat sink is investigated under different angles. Positive and negative orientation of the heat sink have influence on the possible contribution of the gravitational effects. Experimental range includes three angular positions (+30°, 0°, -30°), two mass velocities ( $G=105$  and  $210 \text{ kg m}^{-2} \text{ s}^{-1}$ ) and a large heat flux interval ( $194 - 366 \text{ kW m}^{-2}$ ). Inlet and ambient temperatures are constant at approximately  $T_i = 73^\circ\text{C}$  and  $T_a = 24^\circ\text{C}$ , respectively. It is concluded that optimum thermal performance is got for the horizontal orientation ( $0^\circ$ ) for both the mass flux values. The wetting process as well as balance of the gravitational force (related to liquid flow) and buoyancy force (related to the vapor flow) plays a key role on the thermal performance. Both the relevant forces are related to inclination angle. The pressure drop at the condition of  $\phi = 0^\circ$  is relatively higher than those of the others ( $\phi = +30^\circ$  and  $-30^\circ$ ).

**Keywords:** Angular position, Gravitational effect, Flow boiling, Micro-pin

## 1. Introduction

Among the indispensable parts of devices extensively used in military, space, aviation and health industries, electronic control units play a key role. Also, the critical part of an electronic control unit is a microprocessor including billions of transistors. Even, at present conditions, as underlined by Quhe et al. [1], a conventional microprocessor includes more than 10 billion transistors. In the machines manufactured by Apple, more than 114 billion transistors can be used on a chip [2]. In data centers or supercomputers much more units are banded together. Based on the Moore's Law [3, 4], number of transistors incrementally increase, biennially. From the physical aspect, densely layout of this micro/nano structures in limited volumes causes very high waste heat that must be removed from the working systems [5, 6]. To solve this problem, in micro-pin-fin type heat sinks with flow boiling rise to prominence with also a great potential for future expectations [7]. In recent years, this up-to-date subject has been extensively studied, and results have been reported by ongoing studies.

Lingjian et al. [8] reports experimental results regarding onset of nucleate boiling (ONB) of various heat sinks with different shapes of pins. Circular pins were able to start nucleation at relatively lower heat flux compared to diamond and oval counterparts. Qin et al. [9] focused on the investigation of a heat sink having diamond type micro pins. Contact angle ( $90^\circ$ ,  $120^\circ$  and  $150^\circ$ ) was the main parameter of research. An important report stating that the thermal characteristics of the micro arrays significantly deteriorated with increasing contact angle was declared by them. Ma et al. [10] studied flow boiling in heat sinks having rectangular fins but different fin widths and gaps. Different from the smooth one, the finned surfaces had hydrophobic characteristics, and due to this feature (and reduction of bubble drag), finned surfaces presented lower pressure drop against smooth counterpart. Feng et al. [11] investigated geometrically hybrid (fins + by-pass ways) heat sinks for flow boiling characteristics. Longitudinal gradient by-pass ways were formed between groups of fins. Hybrid geometry prevented or reduced flow reversal of vapor, and therefore increased critical heat flux (CHF). However, compared to uniform pin fin type, uniformity of temperature distribution was deteriorated. Zhou et al. [12] performed experiments in manifold microchannel heat sinks with different topologies. Topology modification improved heat transfer success against conventional heat sink. Huang et al. [13] dealt with behavior of radial micro-pinned heat sinks under hot spot conditions regarding boiling. More stable thermal characteristics were provided compared to those of classic parallel channel heat sink.

Great interest for flow boiling in micro-pinned heat sinks, and importance of them in terms of superior thermal management were summarized above. The subject is in the process of development, and thus, there is a need for novel studies. Different from the literature, as the first time, in this paper, the role of gravitational support/force on flow boiling performance of expanding micro-pin-finned heat sink having staggered fin configuration was investigated. In this regard, three different angles corresponding to  $+30^\circ$ ,  $0^\circ$  and  $-30^\circ$  were considered in the experimental range. Flow images were taken, and underlying physics were discussed via these images in addition to measurement-based graphs.

## 2. Method, Methodology and Experimental Apparatus

The design of the experimental apparatus (see Fig. 1) was organized depending on the flow boiling characteristics. Fluid being filled in a tank was moved in pipes via a micro-pump. The mass flux of deionized water was set to the operational value by using a digital flowmeter and driver of the pump, and temperature of the working fluid was changed when it passed through a heat exchanger (coupled by a constant temperature bath). The inlet temperature of the fluid was adjusted via the preceding process. In brief, the working fluid reached test section at desired temperature. In test section, the fluid was exposed to a specific heat flux via rod type heaters related to an electrical power supply. When temperature values taken throughout the heat sink come to a quasi-steady value ( $\pm 0.5^\circ\text{C}$ ), all the measurement were read. In this regard, instead of temperature measurements, inlet pressure and the total pressure drop (between inlet and outlet plenums of test section) were recorded. Also, via a high-speed camera, images of flow phenomenon were taken. There are two types of operational parameters in the present study: (1) inclination angle and (2) mass flux. Then one of these parameters was changed, and the same procedure was repeated. It should be noted that before each experiment, to get rid of the dissolved gasses, working fluid was vigorously boiled. Details of the degassing procedure and the experimental setup were clearly explained in the earlier articles of the authors, please see some of them as [14, 15].

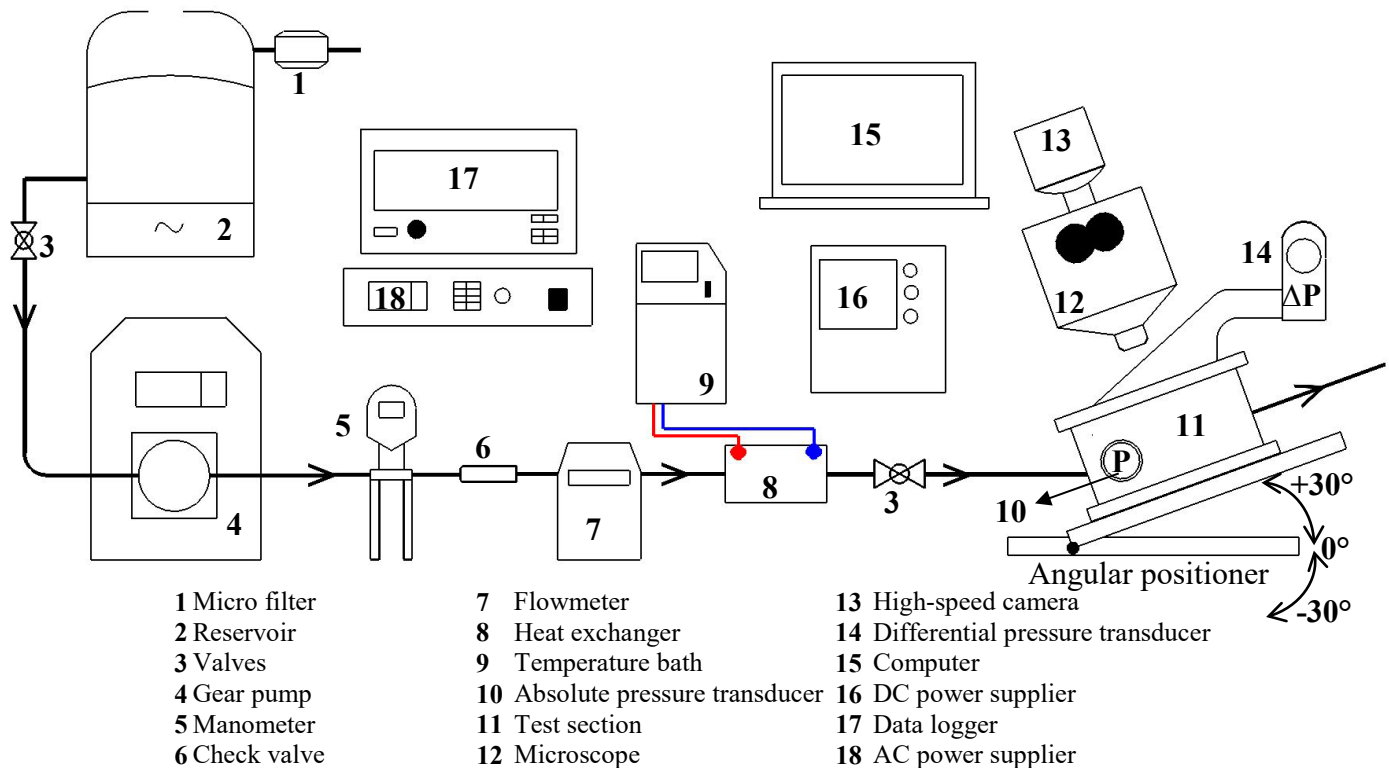


Fig. 1: Experimental setup and devices.

Details of the above-mentioned main (test) section and the exhibition of test piece (heat sink) are exhibited in Fig. 2 and Fig. 3, respectively. The test piece is an expanding type of micro-pin finned heat sink in which fins were oriented in the staggered form. The heat sink is put on the copper block consisting of embedded cartridge heaters connected with AC-power supply. Upper side of the heat sink is covered via a polycarbonate plate (transparent) to form a visible flow duct. Inside first (inlet) chamber, pressure as well as inlet temperature readings are measured. In the outer counterpart, in addition to the existence of a thermocouple for outlet temperature, there is also differential pressure transducer's second branch for total pressure drop measurement. A camera (high-speed type) is utilized to take the images, and data are collected via a datalogger.

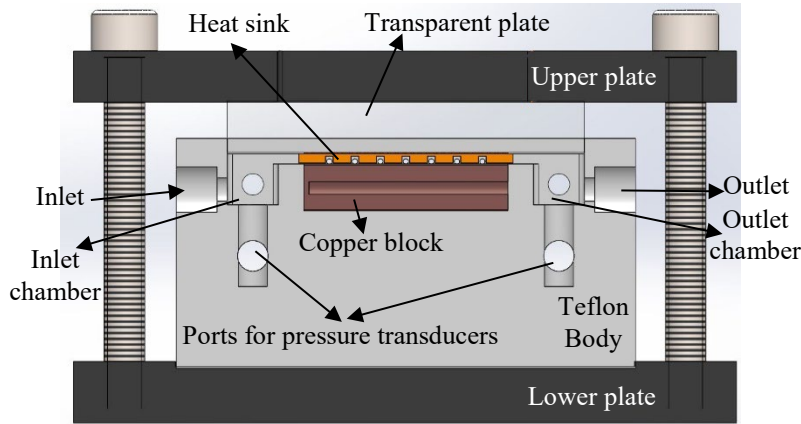


Fig. 2: Test section details.

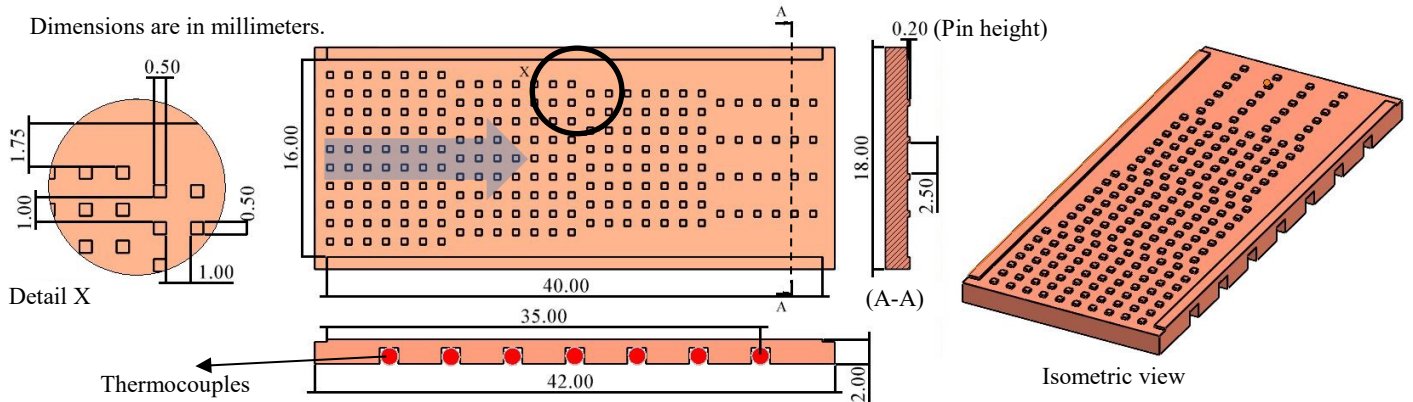


Fig. 3: Heat sink geometry.

Thermal success of a heat sink, for a flow boiling process, may be quantified via heat transfer coefficient, as shown below:

$$h_{tp} = \frac{q_{ap} - q_{loss}}{A_{ts} (T_w - T_{sat})} \quad (1)$$

By subtracting heat loss ( $q_{loss}$ ) from the applied heating power ( $q_{ap}$ ), the heat flux (effective) may be also obtained as in the following way:

$$q_{eff}'' = \frac{q_{ap} - q_{loss}}{A_p} \quad (2)$$

Platform area is demoted by  $A_p$ . Total surface area ( $A_{ts}$ ) is exhibited below:

$$A_{ts} = A_{wf} + \eta N A_f \quad (3)$$

Un-finned area of channel bottom surface of heat sink is demonstrated by  $A_{wf}$ ; while the fin number, fin efficiency and single fin wetted area are symbolized with  $N$ ,  $\eta$ , and  $A_f$ , respectively. On the other hand, local wall temperature and saturation temperature are denoted as  $T_w$  and  $T_{sat}$ , respectively. Explicit forms of all parameters as well as the heat loss equation of heat sink are comprehensively given in previous articles of the authors [14, 16]. The total pressure drop is directly read between inlet and outlet plenums of test section, which is also presented as below:

$$\Delta P = P_i - P_o \quad (4)$$

Where, inlet and outlet are symbolized by the subscripts of  $i$  and  $o$ , respectively. The numerical values of the uncertainties are presented in Table 1. It should be noted that Kline and McClintock's [17] method was utilized regarding uncertainty of the derived parameters.

Table 1: Uncertainty values

Quantity	Uncertainty
$\Delta P$	$\pm 0.08\%$ full-scale
$P_i$	$\pm 0.05\%$ full-scale
$T$	$\pm 0.1$ °C
$q_{ap}$	$\pm 0.6\%$ reading scale
$\dot{V}^*$	$\pm 0.2$ ml min <sup>-1</sup>
$G^*$	$\pm 2.65 - 2.92\%$
$q_{eff}''$	$\pm 2.68 - 2.93\%$
$h_{tp}$	$\pm 1.76 - 11.47\%$

\*  $G$  : Mass flux,  $\dot{V}$  : Volumetric flow rate

### 3. Results and Discussion

In this paper, flow boiling characteristics of an expanding micro-pin-finned heat sink in which fins are oriented in staggered configuration were experimentally investigated at three different inclination angles ( $+30^\circ$ ,  $0^\circ$  and  $-30^\circ$ ). Also, two mass fluxes ( $G=105$  and  $210$  kg m<sup>-2</sup> s<sup>-1</sup>) characterizing relatively low and high values are included in the experimental range. During tests, inlet and ambient temperatures are constant at approximately  $T_i = 73^\circ\text{C}$  and  $T_a = 24^\circ\text{C}$ , respectively. Details of the results are presented below:

In Figure 4, boiling curves that strongly characterizing thermal performance of any flow-boiling-based heat sink are exhibited for both the values of mass flux. For both the mass flux value, the optimum heat transfer performance is got for the horizontal orientation ( $0^\circ$ ). For  $G=105$  kg m<sup>-2</sup> s<sup>-1</sup>, at the inclination angle of  $0^\circ$ , the wall superheat values are lower (up to)  $0.65$  °C and  $1.33$  °C, respectively, compared to the cases of  $\phi = -30^\circ$  and  $\phi = +30^\circ$ . This means that the best cooling can be provided at the horizontal orientation. The relative value of data obtained for  $\phi = -30^\circ$  and  $\phi = +30^\circ$  is strongly depends on mass flux. The probable reason is related to the wetting process as well as balance of the forces acting on flow boiling characteristics, based on the inclination angle. At  $\phi = -30^\circ$ , the gravitational force acts in the same direction with the main flow; however, vapor is forced to perform a reverse flow due to the buoyancy forces. The gravitational force is mainly related to liquid inertia force due to higher density of liquid phase. With increasing mass flux, at the  $\phi = +30^\circ$  the effect of gravitational force acting on liquid film increases and adversely urges the flow motion. However, the rewetting time extends,

more clearly, the time of liquid stays on heat transfer surface increases. Balance of the above-mentioned phenomena influences the obtained results.

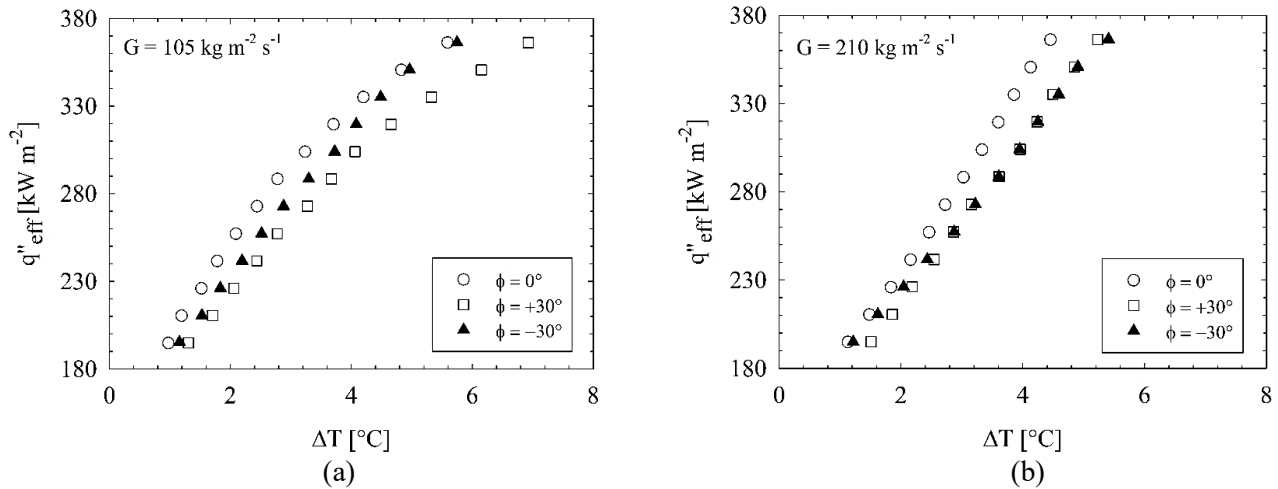


Fig. 4: Boiling curves: for  $G = 105 \text{ kg m}^{-2} \text{ s}^{-1}$  (a) and  $G = 210 \text{ kg m}^{-2} \text{ s}^{-1}$  (b).

The heat transfer results are also presented depending on heat transfer coefficients versus effective heat flux (see Fig. 5). For all cases under consideration,  $h_{tp}$  decreases with increasing value of heat flux. The cases which are at the relatively low heat flux corresponds to early period of saturated boiling; and therefore, active bubble nucleation leads to enhancement of thermal performance. With increasing heat flux number of nucleating bubbles decreases and thus thermal performance deteriorates. The heat transfer coefficients obtained for  $\phi = 0^\circ$  is clearly higher than those of  $\phi = +30^\circ$  and  $\phi = -30^\circ$ . At  $G = 105 \text{ kg m}^{-2} \text{ s}^{-1}$ , the  $h_{tp}$  determined for the condition of  $\phi = 0^\circ$  enhances up to 43.1% and 28.2%, respectively, compared to those of  $\phi = +30^\circ$  and  $\phi = -30^\circ$ . At  $G = 210 \text{ kg m}^{-2} \text{ s}^{-1}$ , the maximum enhancement ratio of the results of  $\phi = 0^\circ$  is 33.7% against the case of  $\phi = +30^\circ$ , and 21.4% compared to the case of  $\phi = -30^\circ$ . At relatively higher mass velocity, the heat transfer coefficients obtained for  $\phi = +30^\circ$  and  $\phi = -30^\circ$  nearly overlaps. The probable reason is related to balance between the gravitational force, the buoyancy force and wetting phenomenon. The details have been already presented in the discussion of the boiling curves.

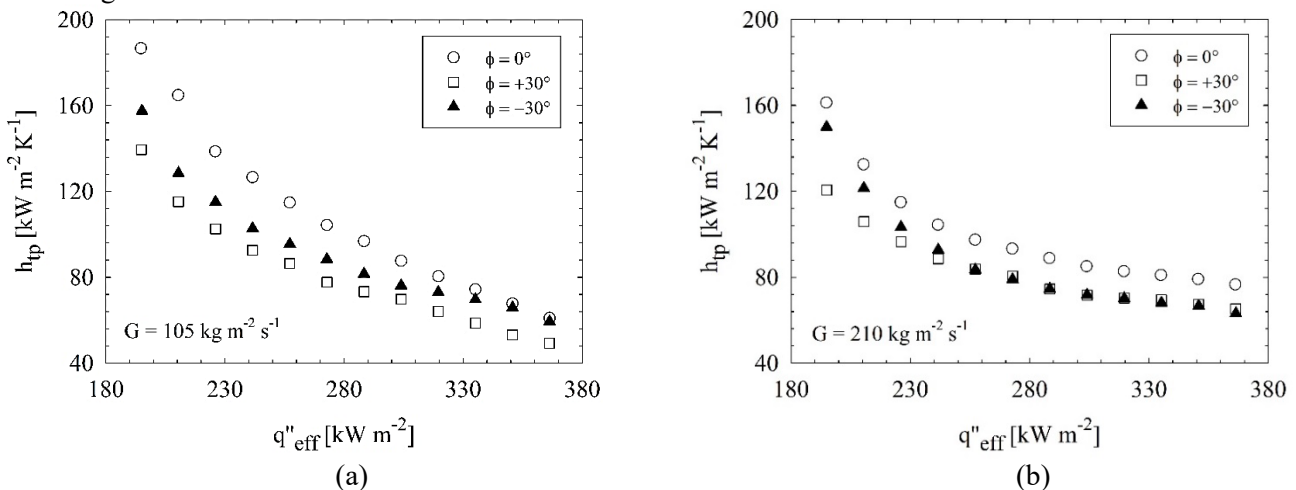


Fig.5: Effect of mass flux on heat transfer coefficients for different inclination angles.

The curves being arranged depending on effect of mass flux is presented in Fig. 6. For all the inclination angles, effect of mass flux strongly depends on heat flux. Up to a value of heat flux, lower mass flux value ( $G = 105 \text{ kg m}^{-2} \text{ s}^{-1}$ ) leads to higher heat transfer coefficients; while at relatively high heat flux values, the greater mass flux presents better thermal performance. However, it should be noted that the transition point changes depending on the inclination angle. From  $\phi = +30^\circ$  to  $-30^\circ$ , the transition postpones to higher heat flux value. At the condition of  $\phi = +30^\circ$ , gravitational force mainly affecting liquid mass or film acts on the reverse direction according to the main flow. This phenomenon extends the wetting time. At relatively low mass flux, the low quantity of liquid easily evaporates, and thus, the heat transfer surface suffers lack of liquid wetting. Increasing mass flux partially prevents this problem. Therefore, due to the above-mentioned flow phenomena, variation of mass flux leads much more influence on the thermal results for  $\phi = +30^\circ$ .

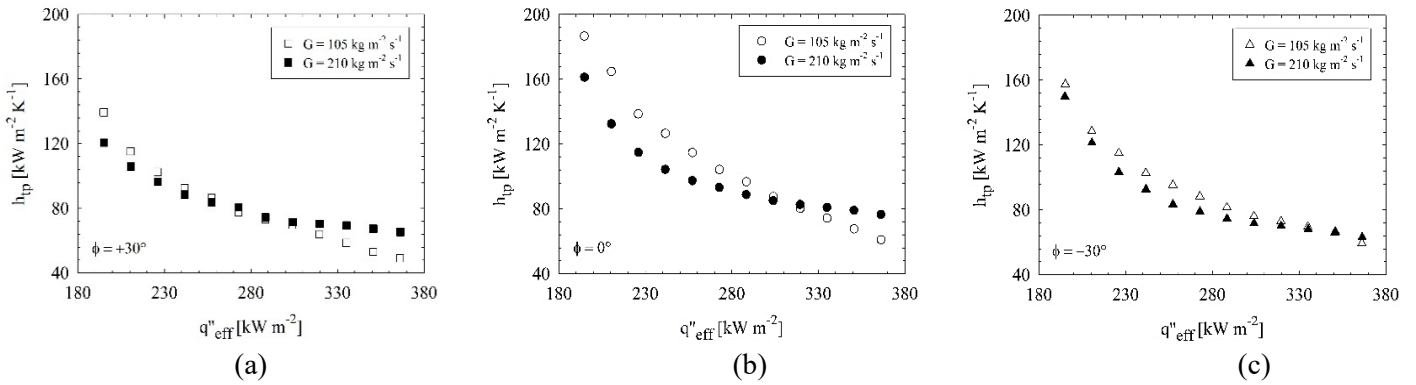


Fig.6: Effect of mass flux on heat transfer coefficients for different inclination angles.

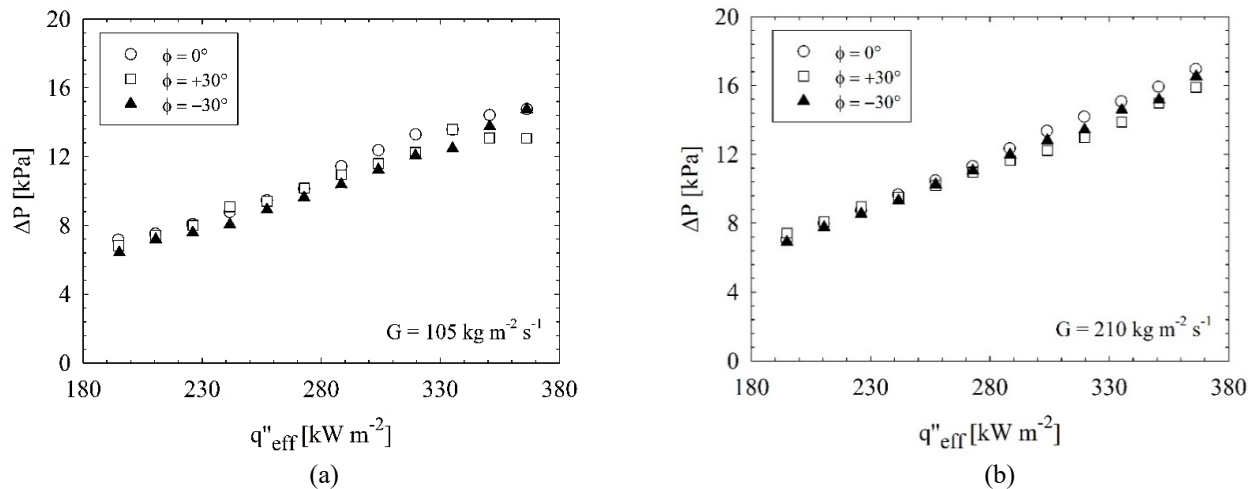
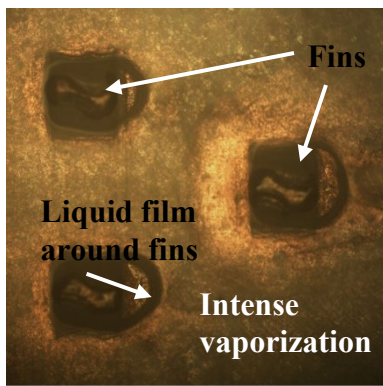


Fig.7: Pressure drop versus effective heat flux for all inclination angles.

In Figure 7, the total pressure drop is presented for all inclination angles. Total pressure drop, in saturated flow boiling conditions, has two components as acceleration and frictional pressure drops. Both of which increase with increasing heat flux; therefore, for all inclination angles, increasing heat flux increases pressure. Pressure drop at the condition of  $\phi = 0^\circ$  is relatively higher than those of the others. The reason is that there is no role of gravitational force or buoyancy force on the flow characteristics contrary to the other conditions. For the inclined conditions ( $\phi = +30^\circ$  and  $-30^\circ$ ), buoyancy force related to the vapor flow and the gravitational force related to the liquid flow act at opposite directions according to each other. Their combined influence leads to the variation on the pressure behavior. To show same flow characteristics, in Fig. 8, flow images are presented for different operational conditions. In Figure 8a, it is seen that vapor covers a large area due to relatively high heating power (220W). And liquid film wrapping the fins is relatively longer (in the flow direction) compared to the  $\phi = 0^\circ$

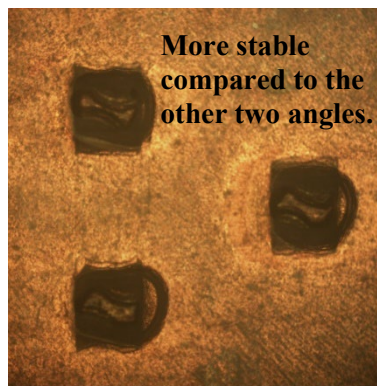
(see Fig. 8b) due to the drag force stemmed from the buoyancy-force-based-moving of the vapor. On the other hand, at  $\phi = -30^\circ$  (see Fig. 8c), the liquid films are longer compared to those of the other angles; and this phenomenon shows the effect of gravitational force on flow physics. In Figure 8d, in the main flow direction, the manipulation of the liquid film by the vapor phase is seen clearer. At the relatively high mass flux condition, the liquid content is much more (compared to Fig. 8a), and thus, the existing liquid is fluctuated by the buoyancy-force-based vapor flow (in the main flow direction). Also, at horizontal position (see Fig. 8e), the liquid content encircling the fins are much more compared to the lower mass flux case (compared to Fig. 8b). On the other hand, in the last image (Fig. 8f) representing the case of  $\phi = -30^\circ$  (and  $G=210 \text{ kg m}^{-2} \text{ s}^{-1}$ ), it is seen that there is a complex flow pattern. At the relevant conditions including relatively high mass flux, liquid flow is supported by the gravitational force in the main flow direction; and the content of liquid in this case is higher than that of Fig. 8c. On the other hand, vapor is exposed to buoyancy force in the opposite direction. Interaction of the relevant forces as well as the drag between the phases induce a segmented flow pattern.

$G=105 \text{ kg m}^{-2} \text{ s}^{-1} \quad \phi=+30^\circ \quad q_{ap}=220 \text{ W}$



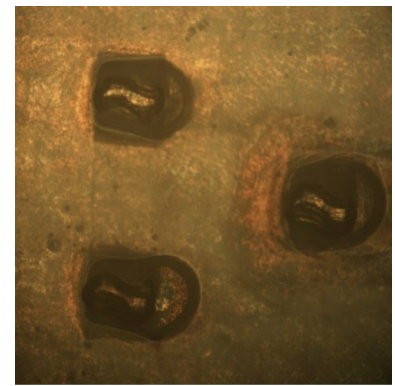
(a)

$G=105 \text{ kg m}^{-2} \text{ s}^{-1} \quad \phi=0^\circ \quad q_{ap}=220 \text{ W}$



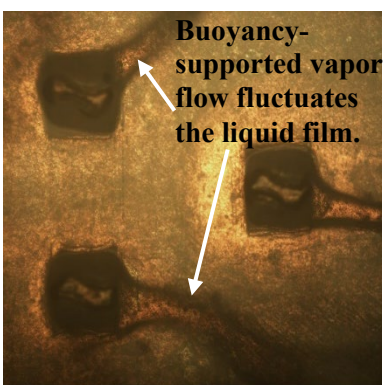
(b)

$G=105 \text{ kg m}^{-2} \text{ s}^{-1} \quad \phi=-30^\circ \quad q_{ap}=220 \text{ W}$



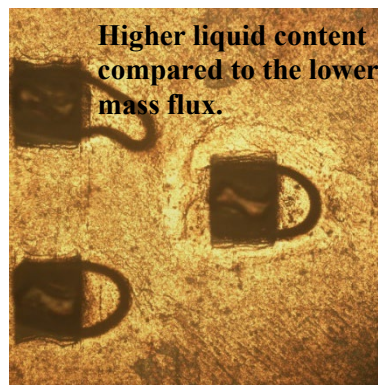
(c)

$G=210 \text{ kg m}^{-2} \text{ s}^{-1} \quad \phi=+30^\circ \quad q_{ap}=220 \text{ W}$



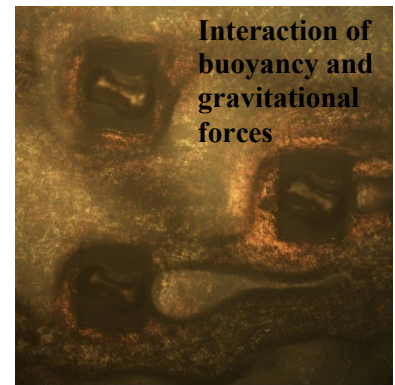
(d)

$G=210 \text{ kg m}^{-2} \text{ s}^{-1} \quad \phi=0^\circ \quad q_{ap}=220 \text{ W}$



(e)

$G=210 \text{ kg m}^{-2} \text{ s}^{-1} \quad \phi=-30^\circ \quad q_{ap}=220 \text{ W}$



(f)

Fig.8: Images taken at 31 mm away from the inlet by a high-speed camera.

#### 4. Conclusion

Here, flow boiling characteristics of expanding micro-fin-finned heat sink were investigated at different inclination angles and mass fluxes. Details were discussed in the previous paragraphs, and a short brief is presented below:

- For both the mass flux values, the best heat transfer characteristics are obtained for horizontal orientation ( $\phi = 0^\circ$ ).
- For  $G=105 \text{ kg m}^{-2} \text{ s}^{-1}$ , at the inclination angle of  $0^\circ$ , the wall superheat values are lower (up to)  $0.65^\circ \text{C}$  and  $1.33^\circ \text{C}$ , respectively, compared to the cases of  $\phi = -30^\circ$  and  $\phi = +30^\circ$ .
- The wetting process as well as balance of the gravitational force (related to liquid flow) and buoyancy force (related to the vapor flow) plays a key role on the thermal performance. Both the relevant forces are related to inclination angle.

- The pressure drop at the condition of  $\phi = 0^\circ$  is relatively higher than those of the others ( $\phi = +30^\circ$  and  $-30^\circ$ ).
- Although the inclination angle has an effect on the results, this effect is limited, as can be seen from the percentage changes. The heat sink can continue the cooling process without entering the critical heat flux at any inclination angle. This is a result of the geometrical superiority of the heat sink.

## Acknowledgement

This paper was performed in the scope of a project supported by TUBITAK. 219M142 is the number of the relevant project. Therefore, we thank the TUBITAK.

## References

- [1] R. Quhe, L. Xu, S. Liu, C. Yang, Y. Wang, H. Li, J. Yang, Q. Li, B. Shi, Y. Li, Y. Pan, X. Sun, J. Li, M. Weng, H. Zhang, Y. Guo, L. Xu, H. Tang, J. Dong, J. Yang, Z. Zhang, M. Lei, F. Pan, J. Lu, "Sub-10 nm two-dimensional transistors: Theory and experiment," *Physics Reports*, vol. 938. Elsevier B.V., pp. 1–72, Nov. 25, 2021. doi: 10.1016/j.physrep.2021.07.006.
- [2] icdrex. (2023, April 25). How many transistors in a computer chip? [Online]. Available: <https://www.icdrex.com/how-many-transistors-in-a-computer-chip/#:~:text=One%20example%20of%20a%20microprocessor,million%20transistors%20per%20square%20millimeter.%20per%20square%20millimeter.>
- [3] G. E. Moore, "Cramming More Components onto Integrated Circuits," in *Proceedings of the IEEE*, vol. 86, no. 1, January 1998.
- [4] Y. Shabany, *Heat Transfer Thermal Management of Electronics*. Taylor & Francis Group, CRC Press, 2010.
- [5] Z. Zhang, L. Jia, and C. Dang, "A Review on Flow Boiling of the Fluid with Lower Boiling Point in Micro-Channels," *Journal of Thermal Science*, vol. 33, no. 1. Science Press, pp. 1–17, Jan. 01, 2024. doi: 10.1007/s11630-023-1885-9.
- [6] S. Kim, S. J. Darges, J. Hartwig, and I. Mudawar, "Assessment and development of saturated and subcooled heat transfer coefficient correlations for cryogenic flow boiling in tubes," *Int J Heat Mass Transf*, vol. 224, Jun. 2024, doi: 10.1016/j.ijheatmasstransfer.2024.125297.
- [7] G. Zhu, S. Liu, D. Zhang, W. Chen, J. Li, and T. Wen, "Transfer learning model to predict flow boiling heat transfer coefficient in mini channels with micro pin fins," *Int J Heat Mass Transf*, vol. 220, Mar. 2024, doi: 10.1016/j.ijheatmasstransfer.2023.125020.
- [8] L. Kong, Z. Liu, L. Jia, M. Lv, and Y. Liu, "Experimental study on flow and heat transfer characteristics at onset of nucleate boiling in micro pin fin heat sinks," *Exp Therm Fluid Sci*, vol. 115, Jul. 2020, doi: 10.1016/j.expthermflusci.2019.109946.
- [9] L. Qin, S. Li, X. Zhao, and X. Zhang, "Experimental research on flow boiling characteristics of micro pin-fin arrays with different hydrophobic coatings," *International Communications in Heat and Mass Transfer*, vol. 126, p. 105456, Jul. 2021, doi: 10.1016/j.icheatmasstransfer.2021.105456.
- [10] X. Ma, X. Ji, J. Wang, X. Yang, Y. Zhang, and J. Wei, "Flow boiling instability and pressure drop characteristics based on micro-pin-finned surfaces in a microchannel heat sink," *Int J Heat Mass Transf*, vol. 195, Oct. 2022, doi: 10.1016/j.ijheatmasstransfer.2022.123168.
- [11] S. Feng, Y. Yan, and C. Lai, "Experimental study on flow boiling characteristics of hybrid micro-channels with gradient distribution pillars and bypass," *Int J Heat Mass Transf*, vol. 186, May 2022, doi: 10.1016/j.ijheatmasstransfer.2021.122468.
- [12] J. Zhou, Q. Li, and X. Chen, "Micro pin fins with topologically optimized configurations enhance flow boiling heat transfer in manifold microchannel heat sinks," *Int J Heat Mass Transf*, vol. 206, Jun. 2023, doi: 10.1016/j.ijheatmasstransfer.2023.123956.
- [13] Y. Huang, Q. Yang, J. Miao, K. Tang, J. Zhao, J. Huang, Y. Guo, "Experimental investigation on flow boiling characteristics of a radial micro pin–fin heat sink for hotspot heat dissipation," *Appl Therm Eng*, vol. 219, Jan. 2023, doi: 10.1016/j.applthermaleng.2022.119622.
- [14] B. Markal and B. Kul, "Combined influence of artificial nucleation site and expanding cross section on flow boiling performance of micro pin fins," *International Communications in Heat and Mass Transfer*, vol. 135, Jun. 2022, doi: 10.1016/j.icheatmasstransfer.2022.106081.
- [15] B. Markal, A. Evcimen, and O. Aydin, "Effect of inlet temperature on flow boiling behavior of expanding micro-pin-fin type heat sinks," *International Communications in Heat and Mass Transfer*, vol. 149, Dec. 2023, doi: 10.1016/j.icheatmasstransfer.2023.107143.
- [16] B. Markal and B. Kul, "Influence of downstream cross-sectional area ratio on flow boiling characteristics of expanding micro pin fin heat sinks," *International Communications in Heat and Mass Transfer*, vol. 143, Apr. 2023, doi: 10.1016/j.icheatmasstransfer.2023.106689.
- [17] S.J. Kline, F.A. McClintock, Describing uncertainties in single-sample experiments. *Mech. Eng.* 75, p3–8, 1953.